Figure Captions

FIGURE 1. Examples of terrain simulations produced by CHILD. Thin solid lines are contours, heavy lines indicate drainage lines, and gray lines show the triangular computational mesh. (A) simulation of gullying on an actual watershed (unnamed watershed on Fort Carson in the foothills of the Colorado Front Range near Colorado Springs). (B) hypothetical fault-bounded mountain range. (C) valley and floodplain development, illustrating meandering stream with variable-resolution mesh. (D) rising mountain block and alluvial fans. Scales in (B), (D), and (D) are nominally 10 km, 1 km, and 2.5 km, respectively.

FIGURE 2. Overview of components in the CHILD model.

FIGURE 3. Elements of the irregular computational mesh, showing nodes (solid circles), triangle edges (black lines), and Voronoi polygons (gray lines). Each Voronoi polygon acts as a finite volume cell. (A) Streamflow is routed downslope from node to node along triangle edges, following the route of steepest descent. (B) Two-dimensional diffusive exchange of sediment between node *N* and its neighbors. The diffusive mass flux per unit width between any two nodes is computed using the gradient between them; multiplying by the width of their shared Voronoi polygon edge gives the total mass exchange rate.

FIGURE 4. Schematic illustration of Poisson rectangular pulse rainfall model (after Eagleson, 1978).

FIGURE 5. Flow chart illustrating the sequence of computations in CHILD.

FIGURE 6. Example of simulated gully erosion and healing in response to stochastic variations in rainfall intensity and duration. Here, a gully system forms and begins to heal on a planar slope (30 degrees, 100 by 100 meters) that is subjected to a series of random storm events. The landscape is highly sensitive to extreme events, owing to a large threshold for runoff erosion (τ_c) and a high soil erodibility coefficient (k_b). (A) Time series of rainfall events (durations not shown). (B) Mean elevation of the surface through time, highlighting the episodic nature of denudation. Arrows indicate the times corresponding to plots C and D. (C) Perspective plot of slope immediately after the last gully-forming episode. (D) Perspective plot at the end of the simulation. (E) and (F) show contour plots at these two time slices. Equation set used in this run is $-dz/dt = 505(\tau - \tau_c)$ (m/yr), with $\tau = 0.62(Q/W)^{2/3}S^{2/3}$ (Pa), τ_c = 20 Pa, and $W = 0.001\,Q^{0.5}$ with Q in m^3/s. Rainfall parameters are $\bar{P} = 0.64$ mm/hr, $\bar{T}_r = 32$ hr, and $\bar{T}_b = 148$ hr; hillslope diffusivity (k_d) is 0.01 m^2/yr.

FIGURE 7. The influence of runoff-production mechanism on terrain morphology. (A) Simulated drainage basin under infiltration-excess (Hortonian) runoff production (Eq (3)). (B) Simulated basin under saturation-excess runoff production, using the O'Loughlin (1986) model (Eq (6)). (C) and (D) plots of surface slope versus contributing area for the two cases. The line in (D) represents the line of saturation for the mean-intensity storm: $S = (\bar{P}/(Tw_v))A$. In these examples runoff erosion is modeled as $-dz/dt = (1.44 \cdot 10^{-5})Q^{0.5}S$. Other parameters are $\bar{P} = 2.9$ mm/hr, $\bar{T}_r = 5$ yr, $\bar{T}_b = 95$ yr, k_d = 0.01 m^2/yr, U = 0.1 mm/yr, and in (B) $T = 1.02 \cdot 10^5$ m^2/yr.

FIGURE 8. Slope-area plots from two simulations illustrating a downstream transition from detachment-limited to transport-limited behavior under (A) constant runoff and (B) variable (stochastic) runoff. Both simulations are in equilibrium with a constant and spatially uniform rate of baselevel fall; the transport and erosion coefficients are adjusted so that the theoretical transition point occurs at the same drainage area in both cases. Although fluvial erosion theory predicts that such a transition should occur in many rivers, the result shown in (B) implies that transitions may be so smooth as to be undetectable in data.

FIGURE 9. Example of a simulated mountain-fan system, showing progradation of a set of alluvial fans in response to block uplift along a vertical fault. The substrate is treated as a cohesionless sediment pile containing a mixture of sand and gravel sediment fractions. Colors indicate the relative proportion of sand in the uppermost (active) sediment layer. (A) 20,000 years after onset of uplift; (B) 40,000 years; (C) 100,000 years. Inset in (C) shows the location of cross-sections in Figure 10. Uplift rate is 1 mm/yr, diffusivity is 0.01 m^2/yr, and rainfall parameters are $\bar{P} = 1.1$ mm/hr, $\bar{T}_r = 3$ yr, and $\bar{T}_b = 97$ yr.

FIGURE 10. Stratigraphic cross-sections through the fan complex in Figure 9. Sections A-C are taken normal to the strike of the range through the center of the fan complex (indicated by a-a' in Figure 9C) (note differences in vertical scales in A, B, C). Color scale for A-C is the same as in Figure 9. (D) shows transverse section at 1 km from the basin edge (b-b' in Figure 9C inset).

FIGURE 11. Illustration of right bank ($\hat{e} = -\hat{n}$) erodibility determination for node *i*. $E_{eff,i1}$ and $E_{eff,i2}$ are effective erodibilities with respect to node *i* at adjacent nodes that are distances, d_1 and d_2, respectively, from the line parallel to the unit vector, $-\hat{n}$. In the coordinate system shown, the *s*-direction is parallel to the flow edge, and the *n*-direction is perpendicular to the flow edge. Delaunay triangulation is in thin solid lines; Voronoi diagram is in dashed lines; and flow edges are in heavy black.

FIGURE 12. Flow chart showing the implementation of meandering.

FIGURE 13. Simulation of channel meandering and floodplain development. (A) Perspective view of simulated topography, highlighting stream pattern and development of terraces. (Elevations are interpolated to regular grid for plotting purposes). (B) View of triangulated mesh, showing densification in the area of the floodplain. (See text for details).

Figure 1

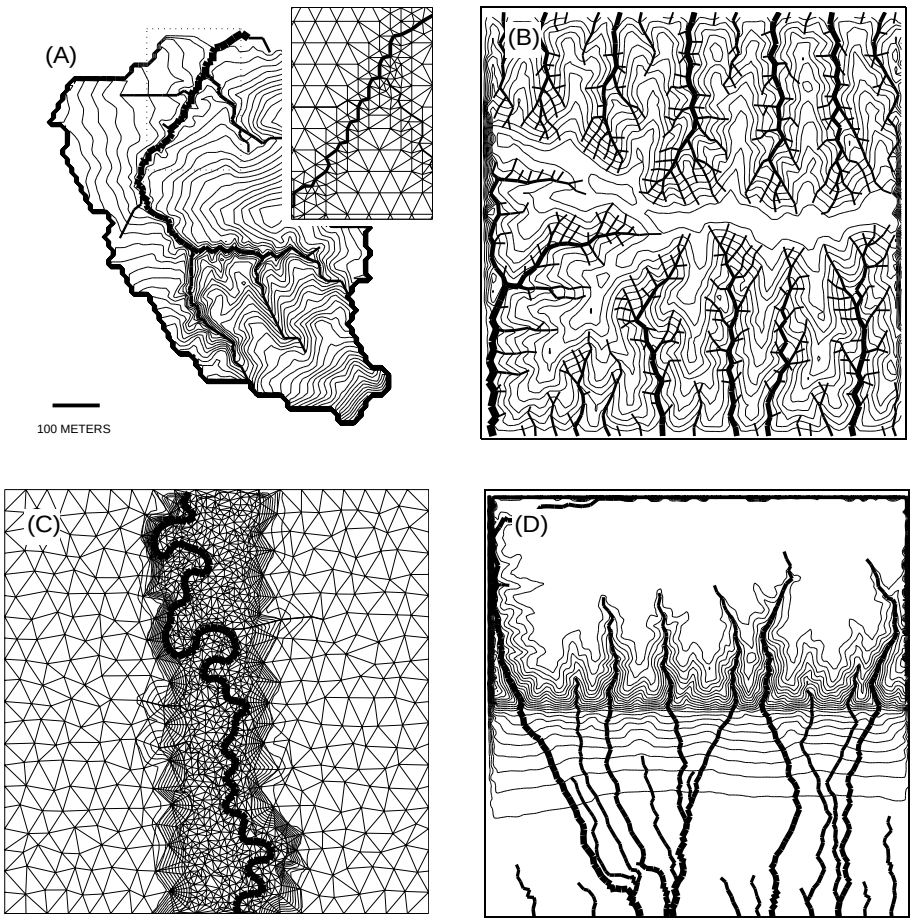

Figure 2

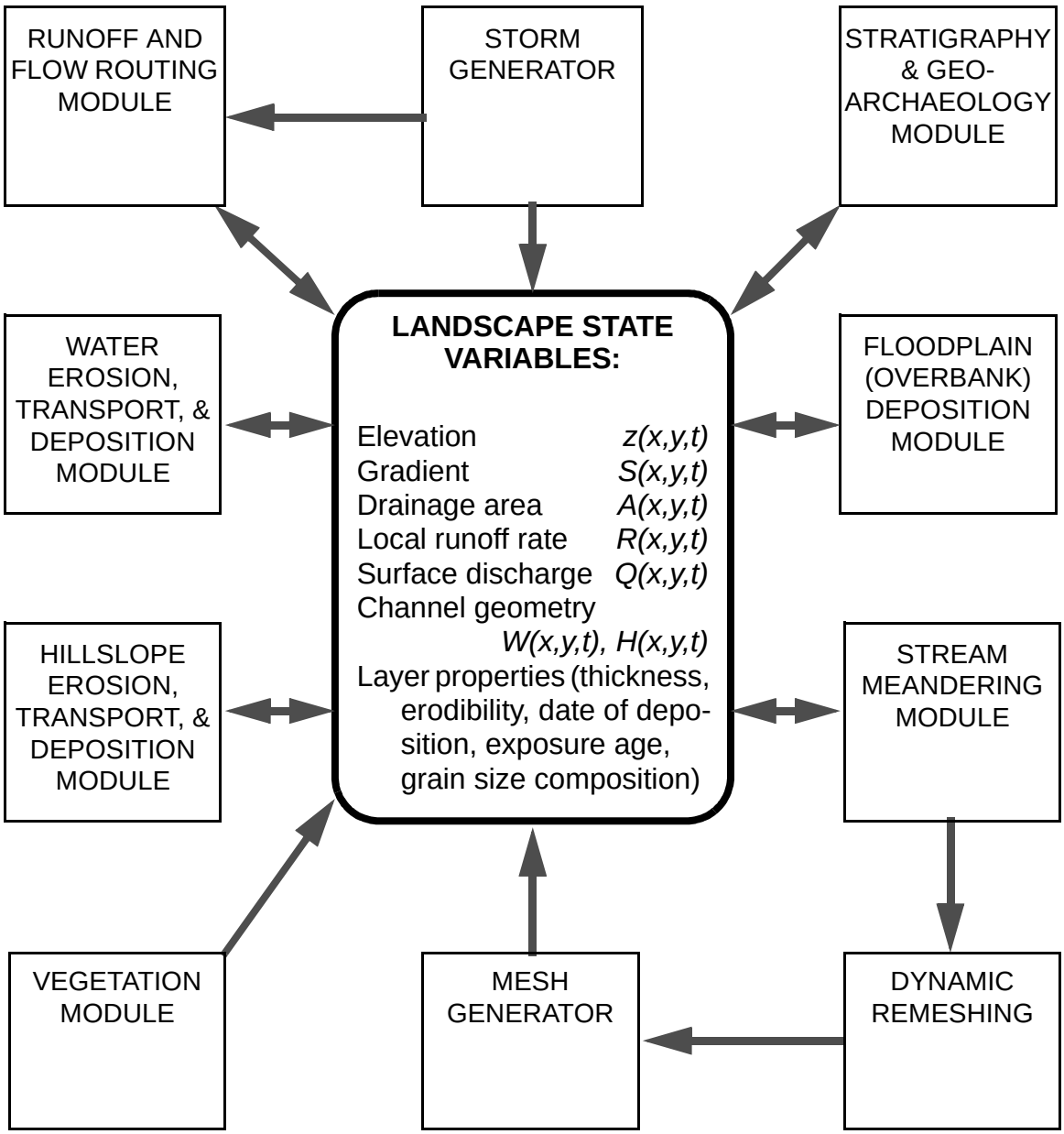
RUNOFF AND FLOW ROUTING MODULE
STORM GENERATOR
STRATIGRAPHY & GEO-ARCHAEOLOGY MODULE
WATER EROSION, TRANSPORT, & DEPOSITION MODULE
LANDSCAPE STATE VARIABLES:
Elevation z(x,y,t)
Gradient S(x,y,t)
Drainage area A(x,y,t)
Local runoff rate R(x,y,t)
Surface discharge Q(x,y,t)
Channel geometry W(x,y,t), H(x,y,t)
Layer properties (thickness, erodibility, date of deposition, exposure age, grain size composition)
FLOODPLAIN (OVERBANK) DEPOSITION MODULE
HILLSLOPE EROSION, TRANSPORT, & DEPOSITION MODULE
STREAM MEANDERING MODULE
VEGETATION MODULE
MESH GENERATOR
DYNAMIC REMESHING

Figure 3

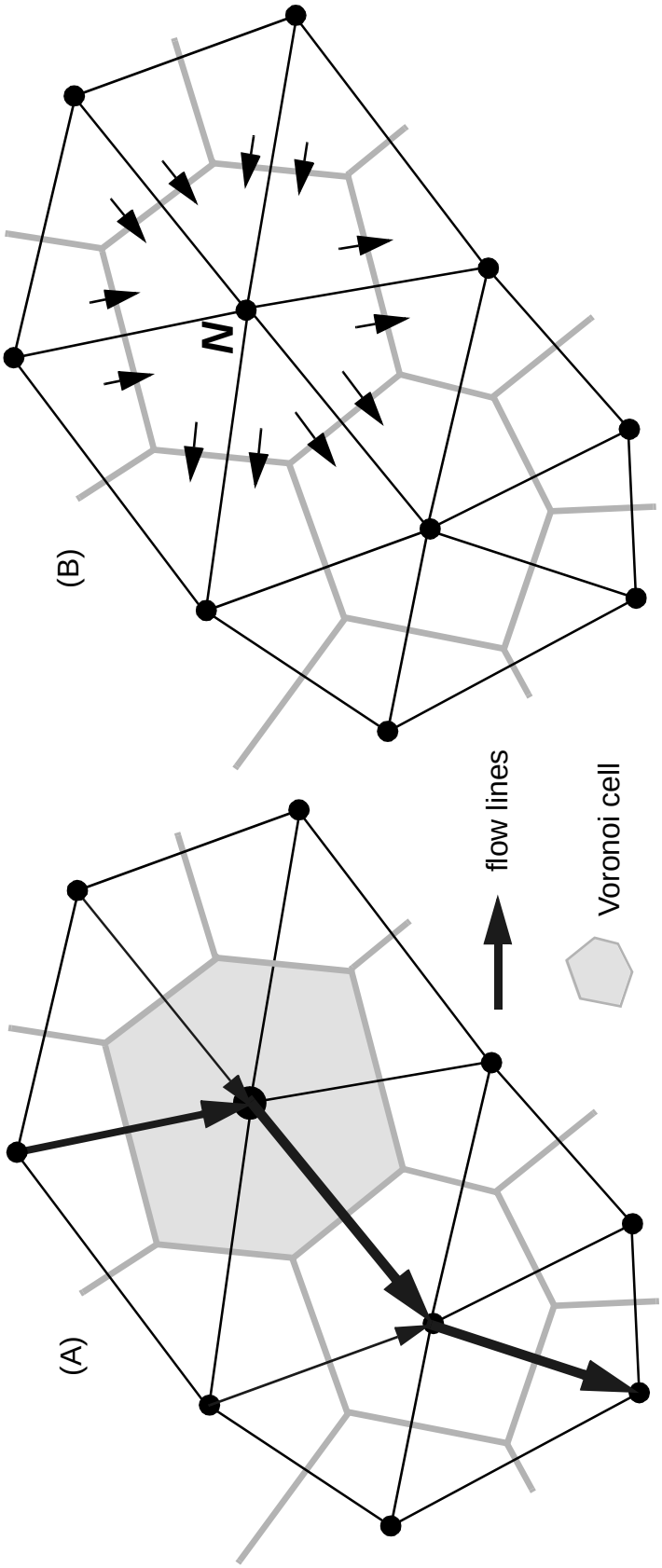

Figure 4

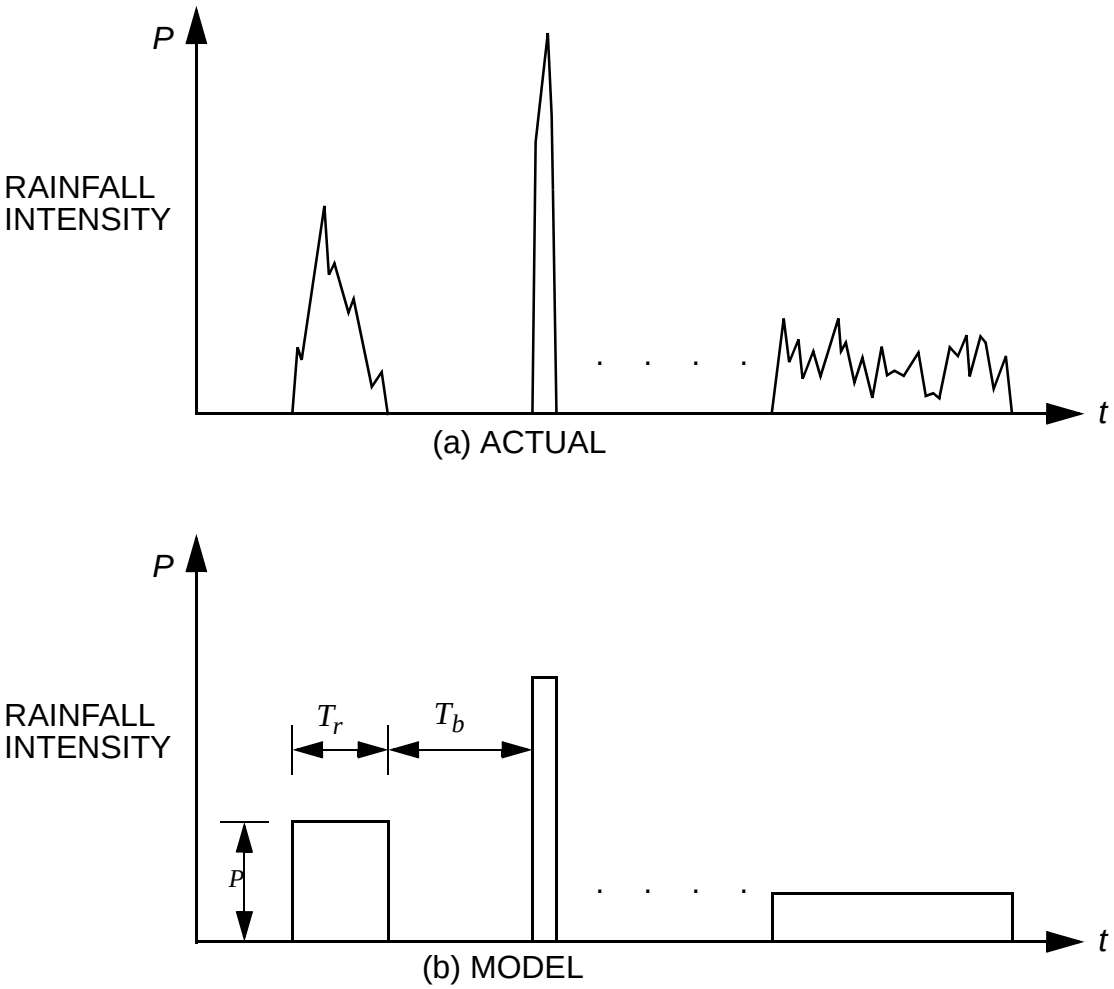
P
RAINFALL
INTENSITY
t
(a) ACTUAL
P
RAINFALL
INTENSITY
T_r
T_b
P
t
(b) MODEL

Figure 5

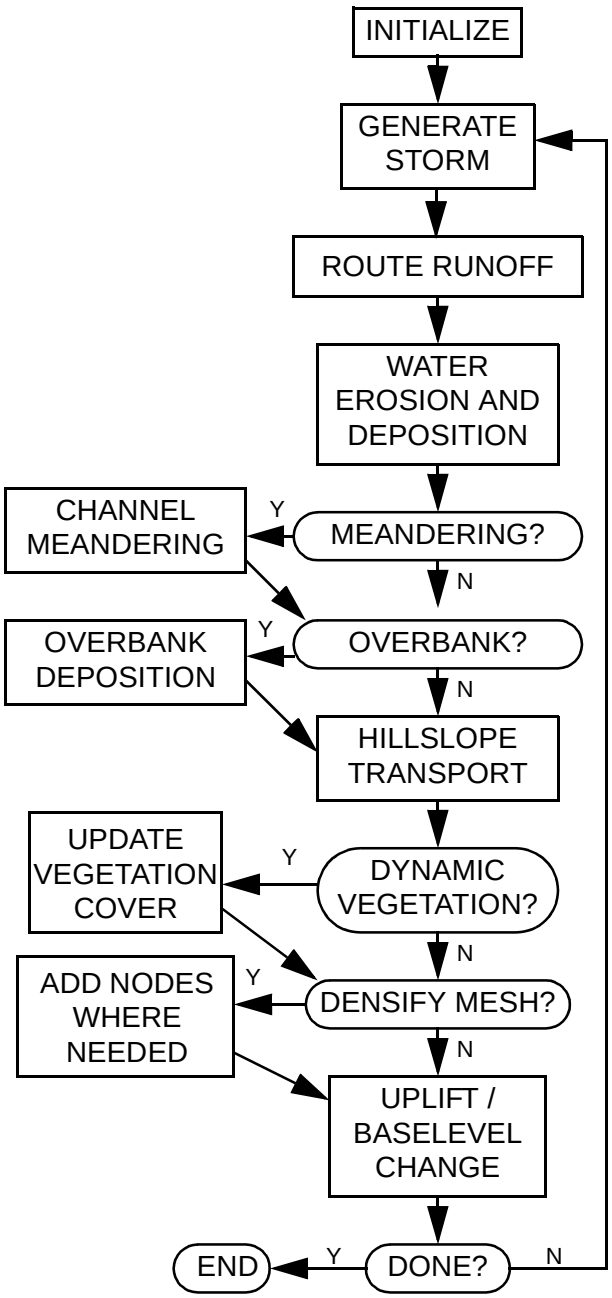
INITIALIZE
GENERATE STORM
ROUTE RUNOFF
WATER EROSION AND DEPOSITION
MEANDERING?
Y
CHANNEL MEANDERING
N
OVERBANK?
Y
OVERBANK DEPOSITION
N
HILLSLOPE TRANSPORT
DYNAMIC VEGETATION?
Y
UPDATE VEGETATION COVER
N
DENSIFY MESH?
Y
ADD NODES WHERE NEEDED
N
UPLIFT / BASELEVEL CHANGE
DONE?
Y
END
N

Figure 6

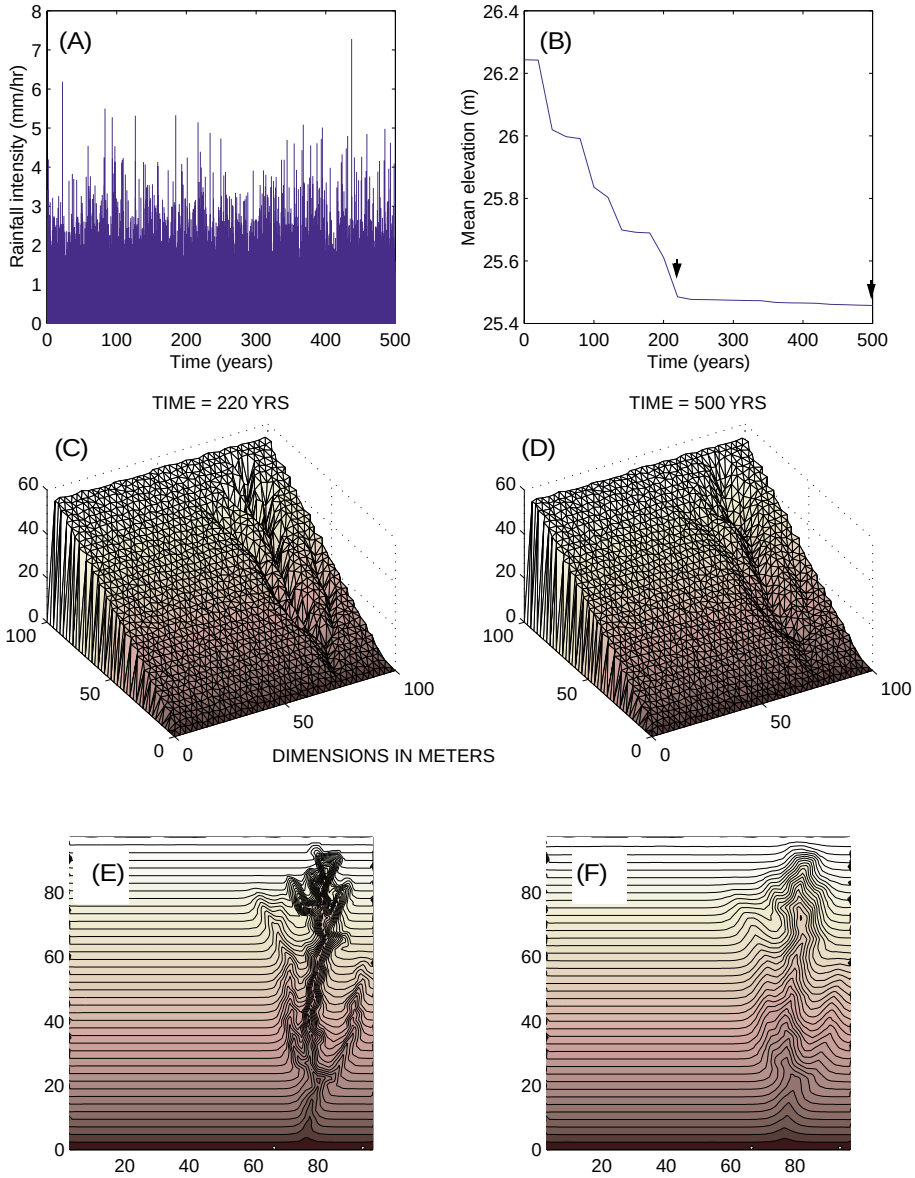
(A)
Rainfall intensity (mm/hr)
Time (years)
(B)
Mean elevation (m)
Time (years)
TIME = 220 YRS
TIME = 500 YRS
(C)
(D)
DIMENSIONS IN METERS
(E)
(F)

Figure 7

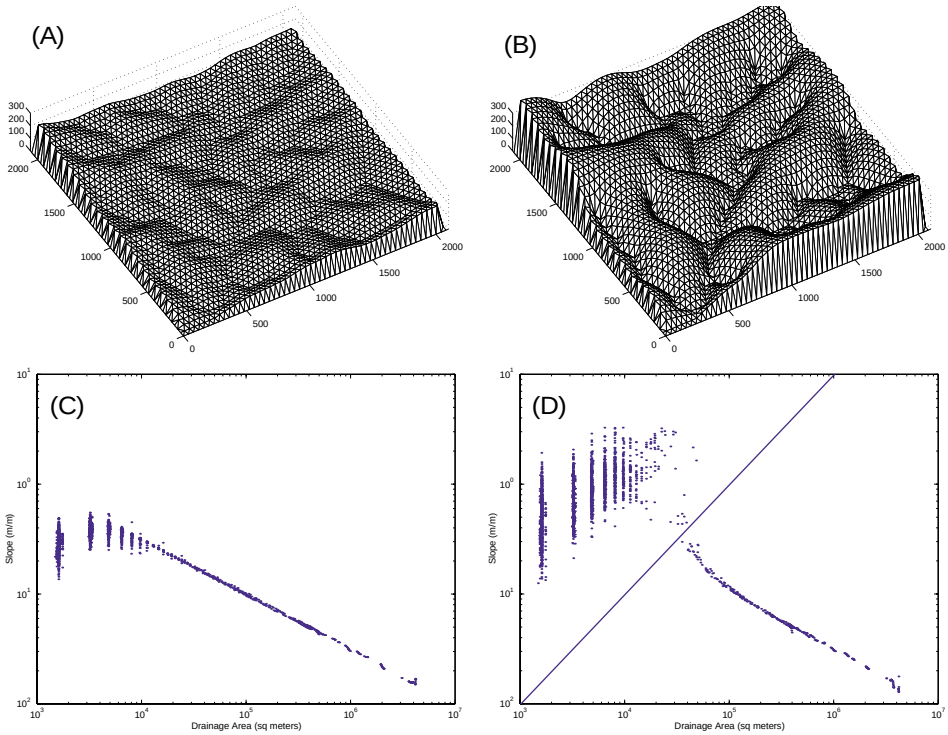

Figure 8

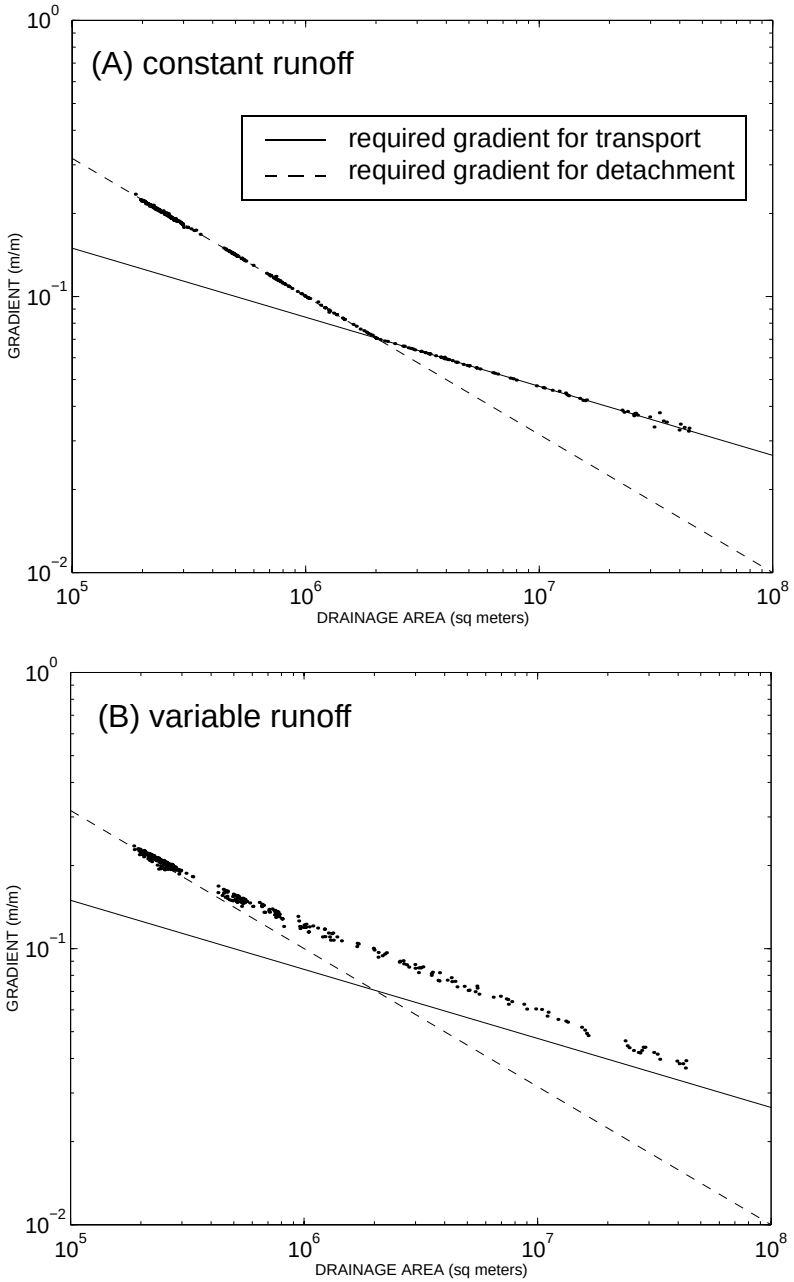
(A) constant runoff
required gradient for transport
required gradient for detachment
GRADIENT (m/m)
DRAINAGE AREA (sq meters)
(B) variable runoff
GRADIENT (m/m)
DRAINAGE AREA (sq meters)

Figure 9a

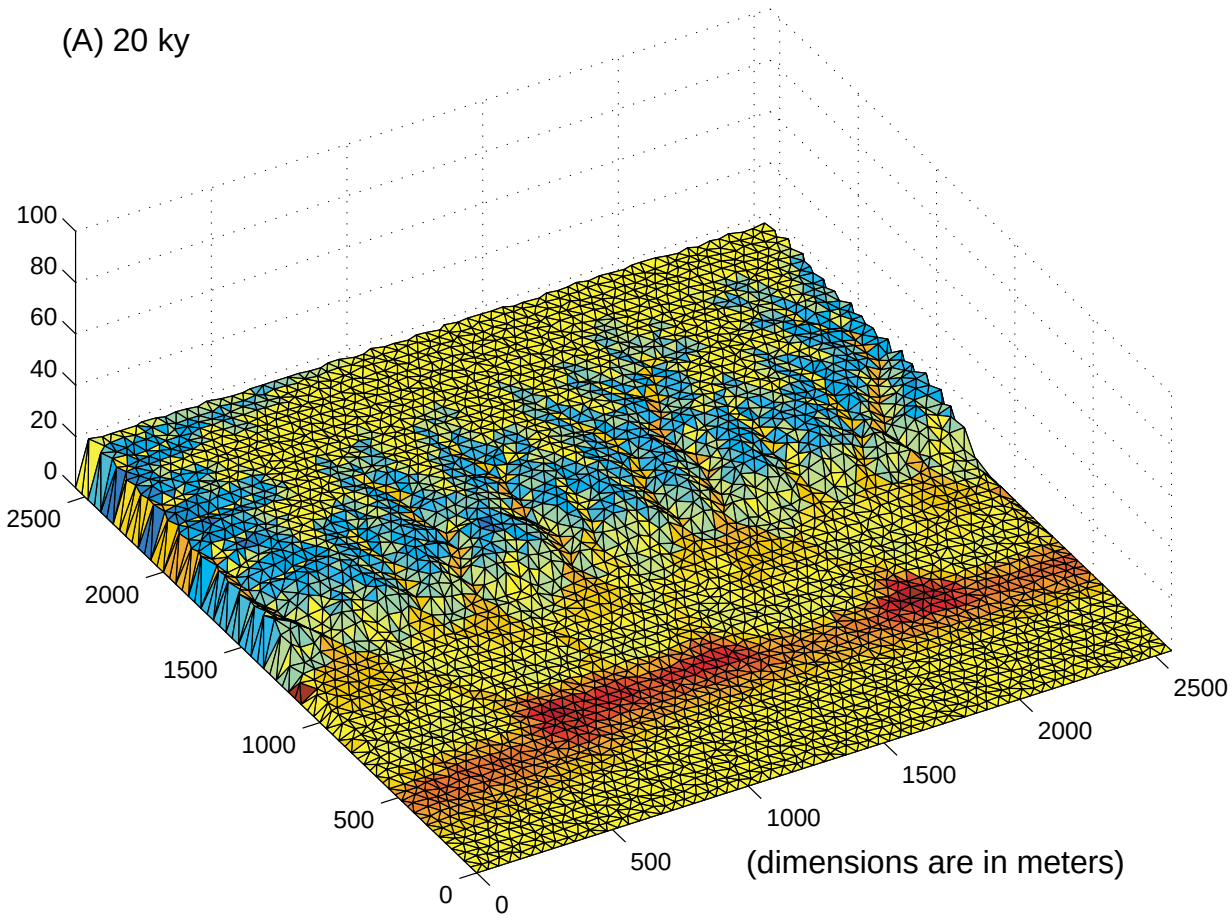
(A) 20 ky
100
80
60
40
20
0
2500
2000
1500
1000
500
0
0
500
1000
1500
2000
2500
(dimensions are in meters)

Figure 9b

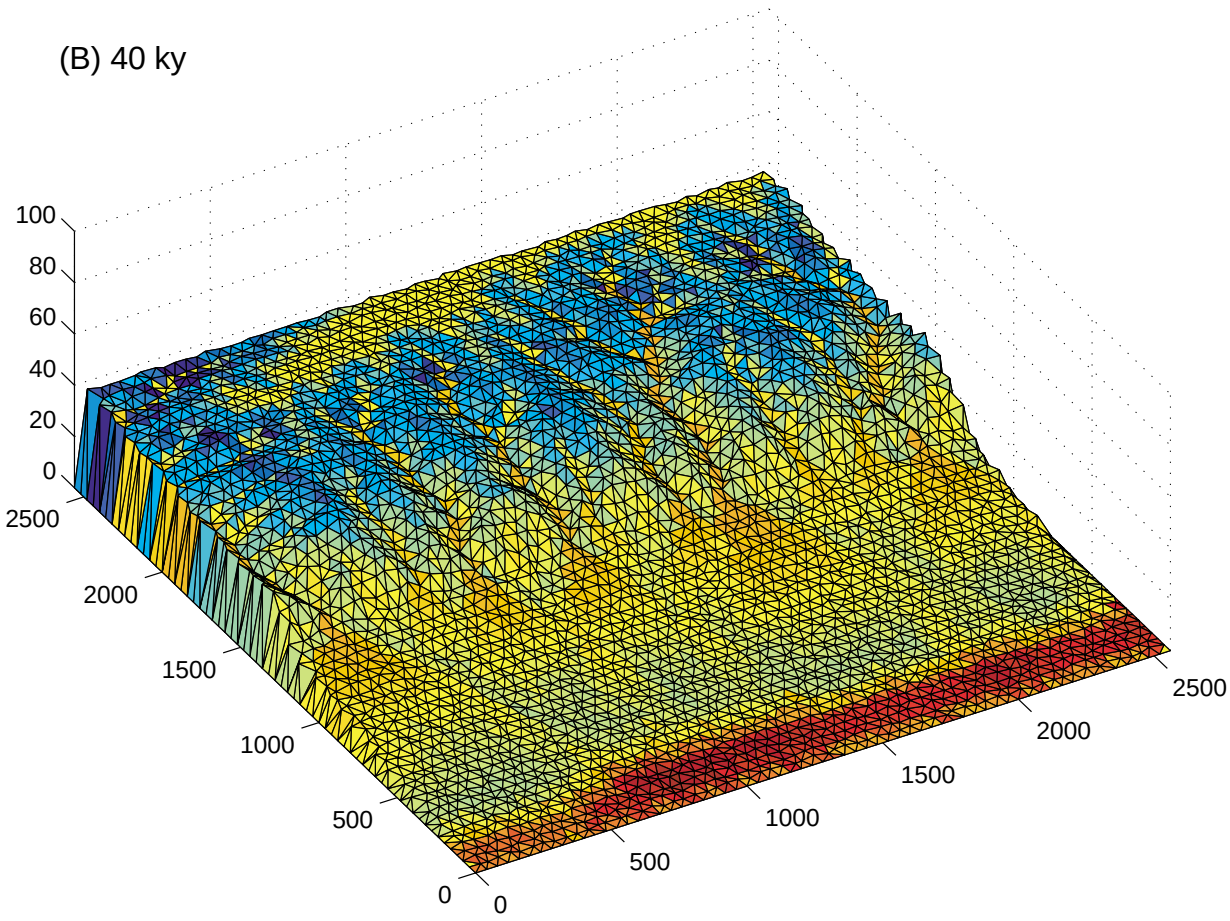
(B) 40 ky
100
80
60
40
20
0
2500
2000
1500
1000
500
0
0
500
1000
1500
2000
2500

Figure 9c

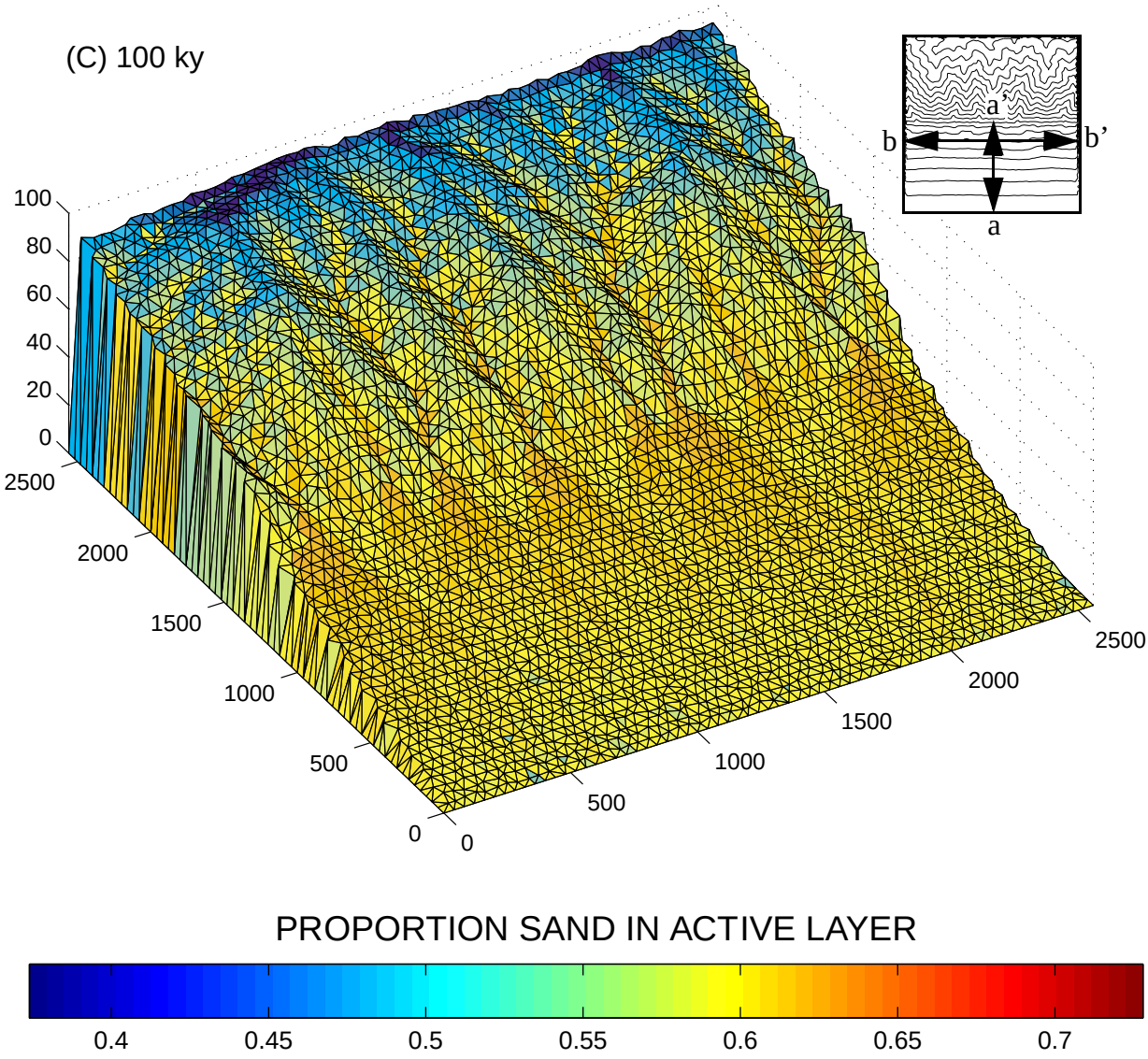
(C) 100 ky
a
a'
b
b'
100
80
60
40
20
0
2500
2000
1500
1000
500
0
0
500
1000
1500
2000
2500
PROPORTION SAND IN ACTIVE LAYER
0.4
0.45
0.5
0.55
0.6
0.65
0.7

Figure 10

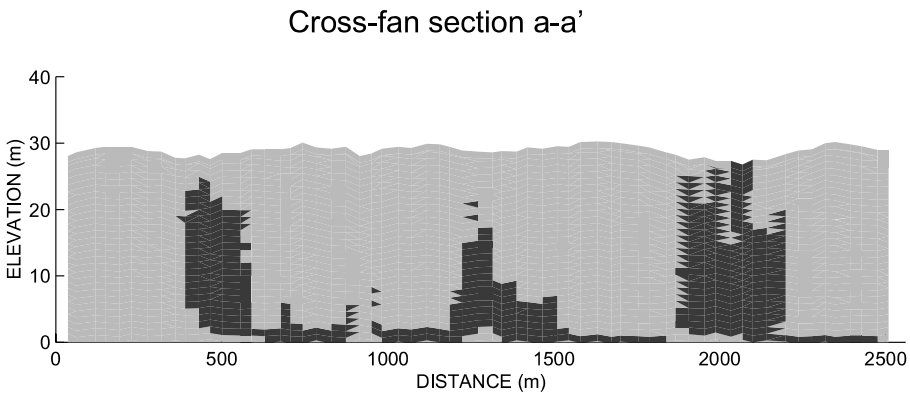
Cross-fan section a-a’
ELEVATION (m)
0
10
20
30
40
0
500
1000
1500
2000
2500
DISTANCE (m)

Figure 11

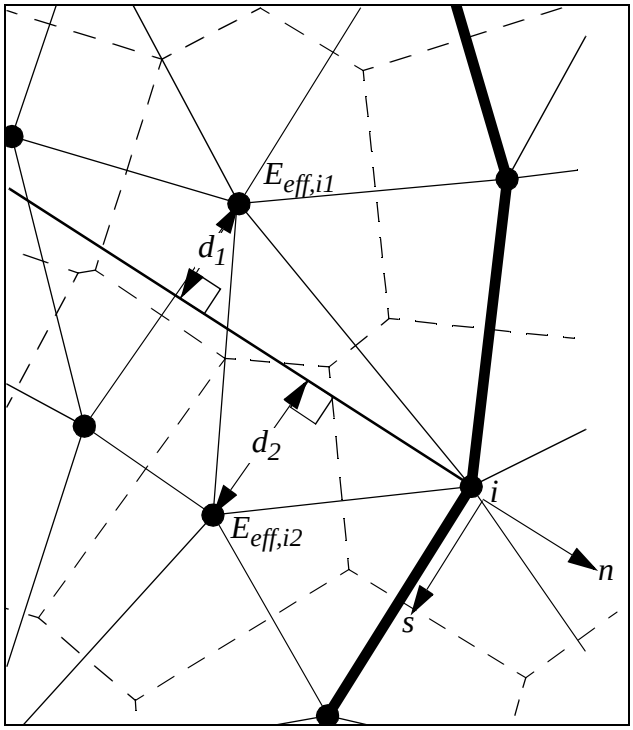

Figure 12

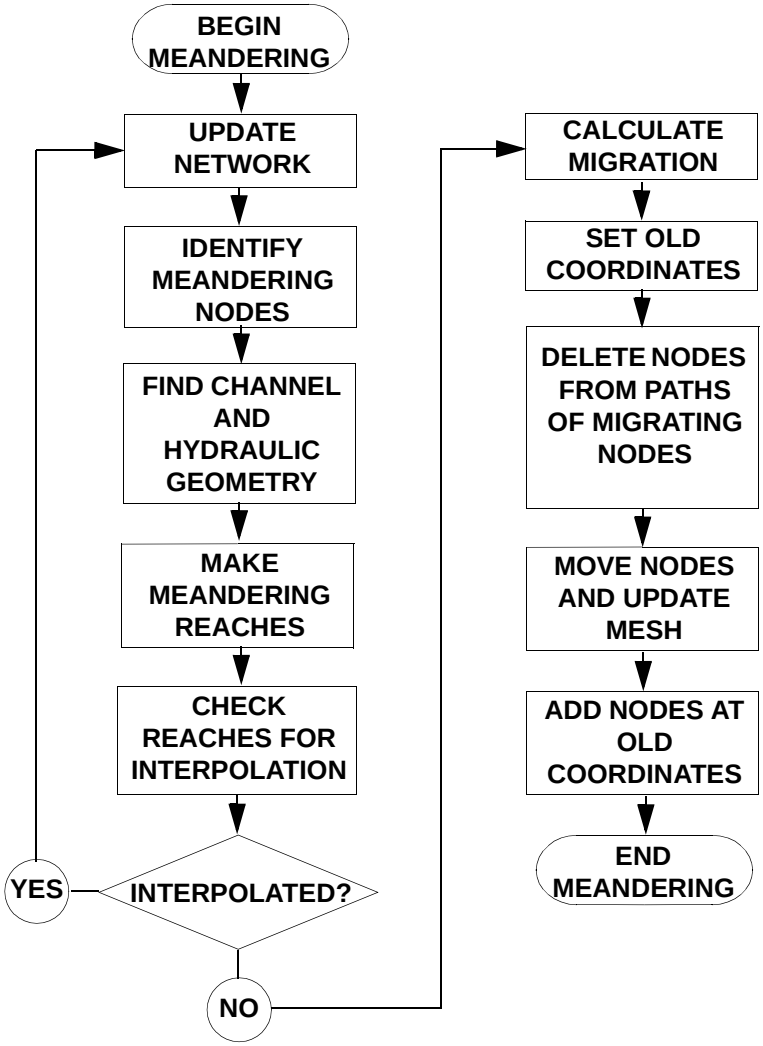
BEGIN MEANDERING
UPDATE NETWORK
IDENTIFY MEANDERING NODES
FIND CHANNEL AND HYDRAULIC GEOMETRY
MAKE MEANDERING REACHES
CHECK REACHES FOR INTERPOLATION
INTERPOLATED?
YES
NO
CALCULATE MIGRATION
SET OLD COORDINATES
DELETE NODES FROM PATHS OF MIGRATING NODES
MOVE NODES AND UPDATE MESH
ADD NODES AT OLD COORDINATES
END MEANDERING

Figure 13

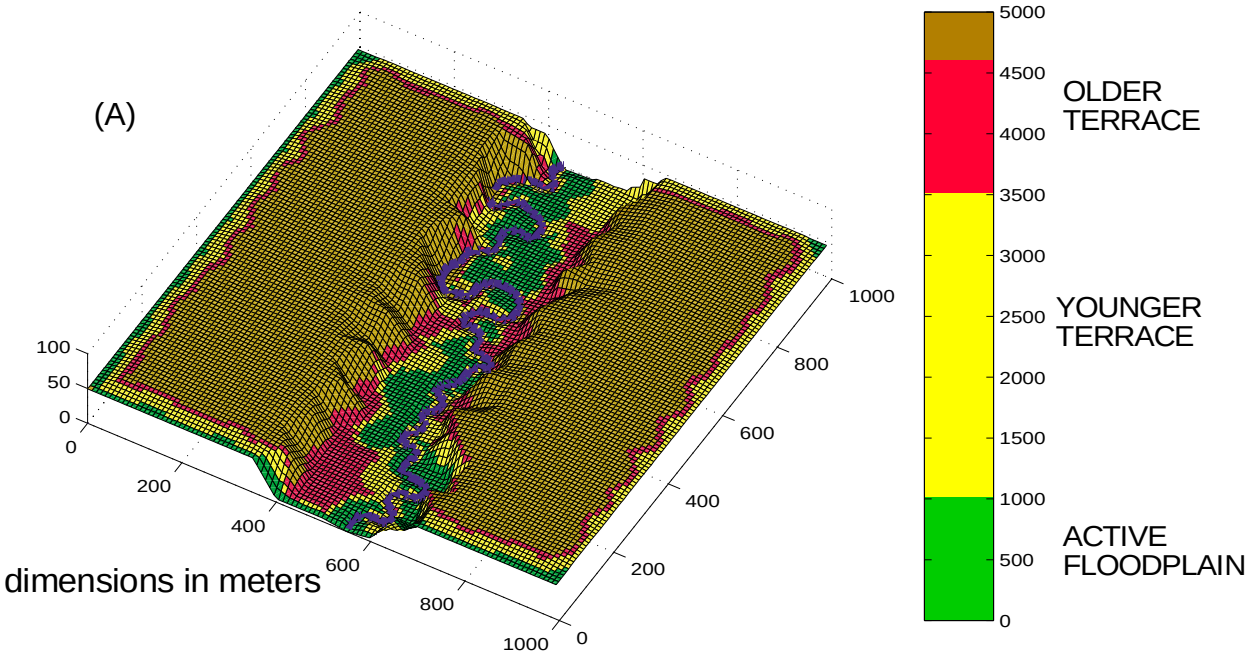
(A)
dimensions in meters
100
50
0
0
200
400
600
800
1000
0
200
400
600
800
1000
5000
4500
4000
3500
3000
2500
2000
1500
1000
500
0
OLDER TERRACE
YOUNGER TERRACE
ACTIVE FLOODPLAIN

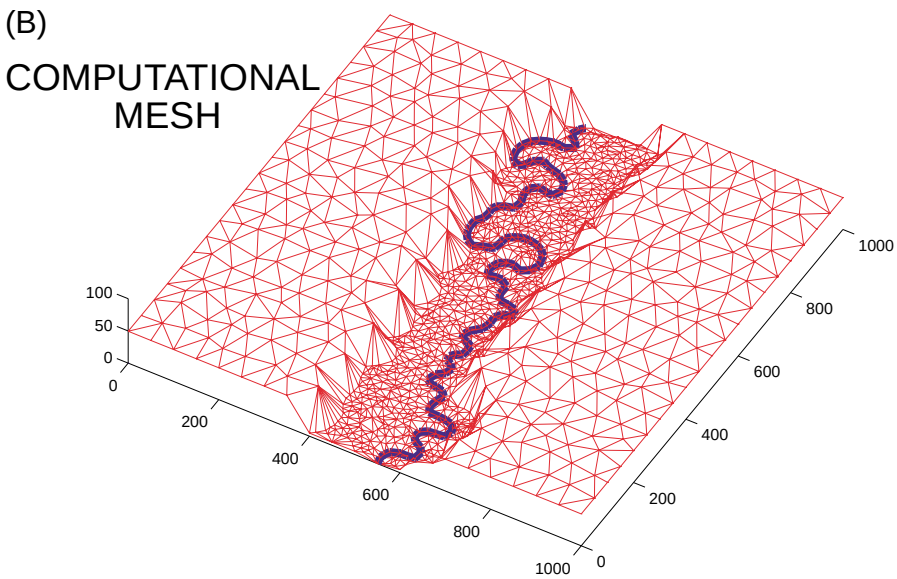
(B)
COMPUTATIONAL MESH
100
50
0
0
200
400
600
800
1000
0
200
400
600
800
1000